arXiv:1211.3182v1 [physics.optics] 14 Nov 2012

Polarization-independent responses of systems with rotational symmetry

Ben Hopkins, Wei Liu, and Andrey E. Miroshnichenko
Nonlinear Physics Centre, Centre for Ultrahigh-bandwidth Devices for Optical Systems (CUDOS), Research School of Physics and Engineering, Australian National University, Canberra, ACT 0200, Australia

For a number of nanophotonic applications, the conditions under which nanoparticle systems have polarization-invariant optical responses remains a largely unresolved issue. We study the optical responses of structures that have an n-fold ($n \geq 3$) rotational symmetry with respect to an axis parallel to the propagation direction of the incident plane wave. Such symmetric systems are considered as constructed from small ($R \ll \lambda$) spherical particles that can be approximated by electric and magnetic dipoles, which allows us to employ the coupled dipole approximation method. It is rigorously proven that all the cross-sections (extinction, scattering and absorption) are independent of the angle of polarization of the linearly-polarized plane wave. It is shown that such polarization-independent responses are purely due to the rotational symmetry of the whole structure and that it is a generic geometric characteristic of any system possessing such symmetry.

PACS numbers: 78.67.-n, 42.25.Fx, 73.20.Mf

I. INTRODUCTION

The current surging interest in various applications of nanoscale light-matter interactions, including biosensing [1–3], nanoantennas [4, 5], photovoltaic devices [6] and many others, has triggered enormous effort into the old and fundamental problem of manipulation of a particle's scattering and absorption characteristics [7, 8]. In the recently emerging fields of nanophotonics, various novel phenomena have been demonstrated involving interaction of nanoparticles with light, such as superscattering [9, 10], control of the direction of the scattered light by metasurfaces [11, 12], coherent perfect absorption of light by surface plasmons [13], Fano resonances in nanoscale structures [14, 15] and plasmonic oligomers[16–22]. At the same time, the interest in artificial magnetic responses that was fostered by the field of metamaterials has lead to the observation of artificial magnetic modes in nanoparticles and, since then, many related novel scattering features based on the interplay of both electric and magnetic responses have been demonstrated [23–29].

To make further breakthroughs in different applications based on the particles scattering, there is a fundamental challenge to overcome: polarization dependence. The dependence of an optical response on polarization comes from the fact that most structures have dominantly electric responses, which are highly dependent on the polarization of the incident field. The simplest structure that does not exhibit polarization-dependent scattering properties is a single spherical particle. According to the Mie theory the total extinction, scattering and absorption cross-sections do not depend on the incident polarization angle, although the scattering diagram will exhibit some angle-dependent properties [7]. However, it is possible to achieve polarization-independent scattering diagram by overlapping of an electric and magnetic dipole responses of a single spherical nanoparticle [28, 29], but such effects can be only achieved by rigorous structure engineering and can happen only in specific spectral regime. It has also been experimentally observed that some plasmonic oligomer structures exhibit polarization-independent extinction cross-sections [19, 30]. This all leads to the question of what the necessary conditions are for an arbitrary system to have polarization-independent scattering properties.

Inspired by the concepts of symmetry induced degenerate states in quantum mechanics [31] and modes degeneracy in uniform waveguides [32–34], there have been some studies about the symmetry-induced polarization-independent scattering by clusters of particles [16, 35, 36]. However, as far as we know, there are no rigorous and systematic investigations of this topic. Additionally, in previous studies, usually only the dependence of extinction or scattering spectra on polarization is investigated and the intrinsic loss spectra is neglected, which could be quite important in its own right, particularly for photovoltaic devices and biological applications.

In this paper we perform a systematic investigation on the optical responses of structures with an n-fold ($n \geq 3$) rotational symmetry, where the n-fold symmetry axis is parallel to the direction of propagation of the incident plane wave [see Fig. 1]. Such n-fold symmetry implies that the optical properties of the system will be identical when rotating the whole structure by $2\pi/n$ radians. But, as we analytically prove, for structures with $n \geq 3$ symmetries the extinction, scattering and even absorption cross-sections are all identical for rotation on *any* angle. Such structures can therefore be considered as being *polarization-independent*.

The extinction and scattering cross-sections are defined in the far-field, but absorption can be calculated by two independent ways - as an energy balance between the far field scattered and incident fields, and as integration of losses in the near field. Both approaches produce the same result. In the near field, the full profile of the electromagnetic field should be taken into account, while in the far field only the leading order will survive. The polarization-independent absorption is then quite counter-intuitive because the near field profile of the electromagnetic field does depend on the incident polarization yet the overall absorption cross-section does not. It implies that the variation of the near field with the incident polarization does not affect the overall integral absorption cross-section. Thus, the near field distribution still follows some symmetry properties of the entire structure. We are able to trace such peculiar relations using the dipole approximation because it is able to show the key aspects of the observed phenomena.

The study in this paper is on symmetric systems consisting of small ($R \ll \lambda$) spherical particles, which can be approximated as electric and magnetic dipoles using coupled dipole approximation [37]. Given that any structure can ultimately be decomposed into small spherical particles and subsequently a composite of electric and magnetic dipoles, the derived polarization-independent response should be a typical feature of any system exhibiting such an n-fold rotational symmetry. As this is a purely geometric feature and shows no dependence on the wavelength, the optical properties of the constituent materials or the resonances excited, we expect that it could be applied in various applications including sensing, imaging, photovoltaic devices and other biological and medical research.

II. THEORETICAL MODEL

A. Discrete dipole approximation

The scattering and absorption of light by a small spherical particle ($R \ll \lambda$) can be approximated by that of an electric and magnetic dipoles with the effective polarizabilities [37]

$$\begin{aligned} \mathbf{p} &= \alpha_E \epsilon_0 \mathbf{E} \\ \mathbf{m} &= \alpha_H \mathbf{H} \end{aligned} \tag{1}$$

where $\mathbf{p}$, $\mathbf{m}$ are the effective electric and magnetic dipole moments, $\mathbf{E}$, $\mathbf{H}$ are the electric and magnetic fields acting on the particle and α_E, α_H are the scalar effective polarizabilities

$$\begin{aligned} \alpha_E &= 6i\pi a_1/k^3 \\ \alpha_H &= 6i\pi b_1/k^3 \end{aligned} \tag{2}$$

as defined here in terms of the Mie dipole scattering coefficients a_1, b_1.

The scattered fields from a single particle in free space can be described in this approximation with dyadic Green's functions

$$\begin{aligned} \mathbf{E^s}(\mathbf{r}) &= k^2 \left[\frac{1}{\epsilon_0} \hat{G}^0(\mathbf{r}, \mathbf{r}_0)\mathbf{p} - \sqrt{\frac{\mu_0}{\epsilon_0}} \left(\nabla \times \hat{G}^0(\mathbf{r}, \mathbf{r}_0) \right) \mathbf{m} \right] \\ \mathbf{H^s}(\mathbf{r}) &= k^2 \left[\hat{G}^0(\mathbf{r}, \mathbf{r}_0)\mathbf{m} + \frac{1}{\sqrt{\epsilon_0 \mu_0}} \left(\nabla \times \hat{G}^0(\mathbf{r}, \mathbf{r}_0) \right) \mathbf{p} \right] \end{aligned} \tag{3}$$

The free space dyadic Green's functions are given by

$$\begin{aligned} \hat{G}^0(\mathbf{r}_i, \mathbf{r}_j) &= \hat{G}^{(3)}_{ij} = a_{ij} \hat{I}^{(3)} + b_{ij} \mathbf{n}_{ji} \otimes \mathbf{n}_{ji} \\ \nabla \times \hat{G}^0(\mathbf{r}_i, \mathbf{r}_j) &= \hat{g}^{(3)}_{ij} = d_{ij} \left(\mathbf{n}_{ji} \otimes \mathbf{n}_{ji} - \hat{I}^{(3)} \right)^{\frac{1}{2}} \end{aligned} \tag{4}$$

in these we have expressed the operator $\mathbf{n}_{ji} \times \hat{I}^{(3)}$ explicitly as $\left(\mathbf{n}_{ji} \otimes \mathbf{n}_{ji} - \hat{I}^{(3)} \right)^{\frac{1}{2}}$ and defined scalars

$$\begin{aligned} a_{ij} &= \frac{e^{ik \cdot r_{ji}}}{4\pi r_{ji}} \left(1 + \frac{i}{k r_{ji}} - \frac{1}{k^2 r_{ji}^2} \right) \\ b_{ij} &= \frac{e^{ik \cdot r_{ji}}}{4\pi r_{ji}} \left(-1 - \frac{3i}{k r_{ji}} + \frac{3}{k^2 r_{ji}^2} \right) \\ d_{ij} &= \frac{e^{ik \cdot r_{ji}}}{4\pi r_{ji}} \left(1 + \frac{i}{k r_{ji}} \right). \end{aligned} \tag{5}$$

where $r_{ji} = |\mathbf{r}_i - \mathbf{r}_j|$ and $\mathbf{n}_{ji} = \frac{1}{r_{ji}} (\mathbf{r}_i - \mathbf{r}_j)$.

In any system constructed from N, small, spherical particles the fields acting on the ith particle will be the sum of both the externally-applied incident fields and the scattered fields from all the other particles. Moreover, by using the expression for scattering from any single particle as given in (3), the expressions for the dipole moments of the ith particle are

$$\begin{aligned} \mathbf{p}_i &= \alpha_{E,i} \epsilon_0 \mathbf{E^0}_i + \alpha_{E,i} \epsilon_0 k^2 \left(\sum_{i \neq j}^{N} \frac{1}{\epsilon_0} \hat{G}^{(3)}_{ij} \mathbf{p}_j - \sqrt{\frac{\mu_0}{\epsilon_0}} \hat{g}^{(3)}_{ij} \mathbf{m}_j \right) \\ \mathbf{m}_i &= \alpha_{H,i} \mathbf{H^0}_i + \alpha_{H,i} k^2 \left(\sum_{i \neq j}^{N} \hat{G}^{(3)}_{ij} \mathbf{m}_j + \frac{1}{\sqrt{\epsilon_0 \mu_0}} \hat{g}^{(3)}_{ij} \mathbf{p}_j \right) \end{aligned} \tag{6}$$

where $\mathbf{E^0}_i = \mathbf{E}^0(\mathbf{r}_i)$, $\mathbf{H^0}_i = \mathbf{H^0}(\mathbf{r}_i)$ are the externally-applied electric and magnetic fields at $\mathbf{r}_i$.

B. Matrix Notation

To describe an entire dipole system we define a state consisting of all dipole moments, $|p\rangle$, and a state consisting the incident fields acting on each dipole, $|e\rangle$

$$\begin{aligned} |p\rangle &= \begin{pmatrix} \mathbf{p}_1 & \cdots & \mathbf{p}_N & \sqrt{\epsilon_0 \mu_0} \mathbf{m}_1 & \cdots & \sqrt{\epsilon_0 \mu_0} \mathbf{m}_N \end{pmatrix} \\ |e\rangle &= \begin{pmatrix} \mathbf{E^0}_1 & \cdots & \mathbf{E^0}_N & \sqrt{\frac{\mu_0}{\epsilon_0}} \mathbf{H^0}_1 & \cdots & \sqrt{\frac{\mu_0}{\epsilon_0}} \mathbf{H^0}_N \end{pmatrix} \end{aligned} \tag{7}$$

where the magnitudes of the magnetic fields and dipole moments in these states have been scaled to be that of the associated electric fields and dipole moments using scaling factors of $\sqrt{\frac{\mu_0}{\epsilon_0}}$ and $\sqrt{\epsilon_0 \mu_0}$.

The dipole equations in (6) show that each incident field vector can be equated to some linear combination of the dipole moments and, as such, there will exist some $6N \times 6N$ matrix, $\hat{M}^{(6N)}$, to relate $|e\rangle$ to $|p\rangle$ as

$$\epsilon_0 \hat{\alpha}^{(6N)} |e\rangle = \hat{M}^{(6N)} |p\rangle . \tag{8}$$

where $\hat{\alpha}^{(6N)}$ is a diagonal matrix containing the electric and magnetic scalar polarizabilities, α_E and α_H, of each particle.

The matrix in (8) is referred to as the *interaction matrix.* To generate a general expression for this matrix, we define four smaller matrices; two that couple electric or magnetic dipoles together, $\hat{M}^{(3N)}_{ee}$ and $\hat{M}^{(3N)}_{hh}$, and two that couple electric to magnetic dipoles and vice versa, $\hat{M}^{(3N)}_{eh}$ and $\hat{M}^{(3N)}_{he}$. These matrices are constructed from the dyadic Green's functions as to match the concatenation of vectors in $|p\rangle$ and $|e\rangle$ [see eq.(7)]

$$\begin{aligned}
\hat{M}^{(3N)}_{ee} &= k^2 \hat{\alpha}_E \hat{M}^{(3N)}_{G} \\
\hat{M}^{(3N)}_{eh} &= -k^2 \hat{\alpha}_E \hat{M}^{(3N)}_{g} \\
\hat{M}^{(3N)}_{hh} &= k^2 \hat{\alpha}_H \hat{M}^{(3N)}_{G} \\
\hat{M}^{(3N)}_{he} &= k^2 \hat{\alpha}_H \hat{M}^{(3N)}_{g}
\end{aligned} \tag{9}$$

where $\hat{\alpha}_{E,H}$ is a diagonal matrix containing the electric or magnetic scalar polarizability of each particle and

$$\hat{M}^{(3N)}_{G} = \begin{pmatrix} \hat{I}^{(3)} & -\hat{G}^{(3)}_{12} & \cdots & -\hat{G}^{(3)}_{1N} \\ -\hat{G}^{(3)}_{12} & \hat{I}^{(3)} & & \vdots \\ \vdots & & \ddots & \\ -\hat{G}^{(3)}_{1N} & \cdots & & \hat{I}^{(3)} \end{pmatrix}$$

$$\hat{M}^{(3N)}_{g} = \begin{pmatrix} \hat{I}^{(3)} & -\hat{g}^{(3)}_{12} & \cdots & -\hat{g}^{(3)}_{1N} \\ \hat{g}^{(3)}_{12} & \hat{I}^{(3)} & & \vdots \\ \vdots & & \ddots & \\ \hat{g}^{(3)}_{1N} & \cdots & & \hat{I}^{(3)} \end{pmatrix} .$$

The interaction matrix that satisfies (8) is then constructed as

$$\hat{M}^{(6N)} = \begin{pmatrix} \hat{M}^{(3N)}_{ee} & \hat{M}^{(3N)}_{eh} \\ \hat{M}^{(3N)}_{he} & \hat{M}^{(3N)}_{hh} \end{pmatrix} . \tag{10}$$

III. POLARIZATION INVARIANCE AND SYMMETRY

A. Rotations and Cyclic Symmetry

In this section we are going to consider particle systems that have a rotational symmetry described by an *n-fold axis.* An *n-fold axis* is an axis in our system about which any number of $\frac{2\pi}{n}$ rotations will leave the system unchanged. This sort of symmetry is also referred to as cyclic symmetry.

In the coupled dipole equation (8) any rotational symmetry must be contained within the set of dyadic Green's functions ($\hat{G}^{(3)}_{ij}$ and $\hat{g}^{(3)}_{ij}$) that make up the interaction matrix as no other terms contain information on the structure of the system. As such we are able to consider only the dyadic Green's functions when applying a general rotation operator, $\hat{R}^{(3)}$, to the position vector of every particle. Moreover, it is only the unit-dyad terms in $\hat{G}^{(3)}_{ij}$ and $\hat{g}^{(3)}_{ij}$ that are affected because the coefficients, a_{ij}, b_{ij} and d_{ij}, are all independent of the position vector directions [see eqs.(4) and (5)]. Explicitly, it follows from the definitions in (4) that both $\hat{G}^{(3)}_{ij}$ and $\hat{g}^{(3)}_{ij}$ will transform as a change of basis under any rotation applied to the system's position vectors

$$\begin{aligned}
\hat{G}^{(3)}_{ij} &\rightarrow \hat{R}^{(3)} \hat{G}^{(3)}_{ij} \left(\hat{R}^{(3)}\right)^T \\
\hat{g}^{(3)}_{ij} &\rightarrow \hat{R}^{(3)} \hat{g}^{(3)}_{ij} \left(\hat{R}^{(3)}\right)^T .
\end{aligned} \tag{11}$$

In order for (11) to follow for the case of $\hat{g}^{(3)}_{ij}$, we must also acknowledge that $\hat{g}^{(3)}_{ij}$ can always be expanded as a Taylor series. This is true because the magnitude of every component in $\left(\mathbf{n}_{ji} \otimes \mathbf{n}_{ji} - \hat{\mathbf{I}}\right)$ will be less than or equal to one and therefore the Taylor series for $\left(\mathbf{n}_{ji} \otimes \mathbf{n}_{ji} - \hat{\mathbf{I}}\right)^{\frac{1}{2}}$, and hence $\hat{g}^{(3)}_{ij}$, will always converge.

So, given that (11) holds for all $\hat{G}^{(3)}_{ij}$ and $\hat{g}^{(3)}_{ij}$, the entire interaction matrix will transform in an equivalent manner

$$\hat{M}^{(6N)} \; \rightarrow \; \hat{R}^{(6N)} \hat{M}^{(6N)} \left(\hat{R}^{(6N)}\right)^T \tag{12}$$

where $\hat{R}^{(6N)}$ is defined such that it applies $\hat{R}^{(3)}$ to the position vector of every particle in $\hat{M}^{(6N)}$

$$\hat{R}^{(6N)} = \hat{R}^{(3)} \hat{I}^{(6N)}. \tag{13}$$

However, for the case of a symmetric rotation about the n-fold axis, $\hat{R}^{(3)}_n$, it also follows that

$$\hat{R}^{(3)}_n \mathbf{r}_{i,j} = \mathbf{r}_{k,l} \tag{14}$$

for each $i,j \in \{1,...N\}$ and $k,l \in \{1,...N\}$. Subsequently the dyadic Green's functions will also transform as

$$\begin{aligned}
\hat{R}^{(3)}_n \hat{G}^{(3)}_{ij} \left(\hat{R}^{(3)}_n\right)^T &= \hat{G}^{(3)}_{kl} \\
\hat{R}^{(3)}_n \hat{g}^{(3)}_{ij} \left(\hat{R}^{(3)}_n\right)^T &= \hat{g}^{(3)}_{kl}
\end{aligned} \tag{15}$$

Therefore there must exist some permutation matrix, $\hat{\Pi}_n^{(6N)}$, for each $\hat{R}_n^{(3)}$ such that

$$\hat{R}_n^{(6N)}\hat{M}^{(6N)}\left(\hat{R}_n^{(6N)}\right)^T = \left(\hat{\Pi}_n^{(6N)}\right)^T \hat{M}^{(6N)}\hat{\Pi}_n^{(6N)}. \quad (16)$$

We can consider all non-zero components of $\hat{\Pi}_n^{(6N)}$ as $\hat{I}^{(3)}$ matrices and therefore $\hat{\Pi}_n^{(6N)}$ will commute with $\hat{R}_n^{(6N)}$. From (16), it then follows that $\hat{R}_n^{(6N)}\hat{\Pi}_n^{(6N)}$ will commute with the interaction matrix

$$\hat{R}_n^{(6N)}\hat{\Pi}_n^{(6N)}\hat{M}^{(6N)} = \hat{M}^{(6N)}\hat{R}_n^{(6N)}\hat{\Pi}_n^{(6N)}. \quad (17)$$

If we also only consider incident fields that do not break the symmetry of the system, that is; fields such that both $\mathbf{e}_i = \mathbf{e}_k$ and $\mathbf{h}_i = \mathbf{h}_k$ for all $i, k \in \{1, ...N\}$ where $\hat{R}_n^{(3)}\mathbf{r}_i = \mathbf{r}_k$, then

$$\hat{\Pi}_n^{(6N)}\left|e\right\rangle = \left|e\right\rangle. \quad (18)$$

The dipole moments of a symmetry-rotated incident field can then be defined as a result of both (17) and (18). Specifically, for some $|e\rangle$, $|p\rangle$ such that $\epsilon_0\hat{\alpha}^{(6N)}\left|e\right\rangle = \hat{M}^{(6N)}\left|p\right\rangle$,

$$\epsilon_0\hat{\alpha}^{(6N)}\left(\hat{R}_n^{(6N)}\left|e\right\rangle\right) = \hat{M}^{(6N)}\left(\hat{R}_n^{(6N)}\hat{\Pi}_n^{(6N)}\left|p\right\rangle\right). \quad (19)$$

A particular subset of incident fields that will obey the result in (19) are the linearly-polarized plane waves travelling parallel to the n-fold axis of our system. To construct a general linearly-polarized wave we consider some orthonormal basis of two plane waves that are in-phase, $|e_h\rangle$ and $|e_v\rangle$. Then any linearly-polarized incident field can be expressed as

$$\left|e\right\rangle = \alpha\left|e_h\right\rangle + \beta\left|e_v\right\rangle; \qquad (\alpha, \beta \in \mathbf{R}). \quad (20)$$

However, if the n-fold axis of our system satisfies $n > 2$, we can choose $\hat{R}_n^{(3)}$ to be a rotation of $\frac{2\pi}{n}$ about the n-fold axis and then express the incident field in an alternate basis of $\left\{\left|e_h\right\rangle, \hat{R}_n^{(6N)}\left|e_h\right\rangle\right\}$ where

$$\left|e_v\right\rangle = a\left|e_h\right\rangle + b\hat{R}_n^{(6N)}\left|e_h\right\rangle; \qquad (a, b \in \mathbf{R}). \quad (21)$$

The prescribed orthonormality of the original basis states, $|e_h\rangle$ and $|e_v\rangle$, requires that

$$\langle e_v|e_v\rangle = a^2 + 2ab\cos(\frac{2\pi}{n}) + b^2 = 1 \quad (22)$$

$$\langle e_v|e_h\rangle = a + b\cos(\frac{2\pi}{n}) = 0. \quad (23)$$

In this basis the general form of any, linearly-polarized, incident field becomes

$$\left|e\right\rangle = (\alpha + \beta a)\left|e_h\right\rangle + \beta b\hat{R}_n^{(6N)}\left|e_h\right\rangle \quad (24)$$

and we can use the relation in (19) to express the associated dipole moments as

$$\left|p\right\rangle = (\alpha + \beta a)\left|p_h\right\rangle + \beta b\hat{R}_n^{(6N)}\hat{\Pi}_n^{(6N)}\left|p_h\right\rangle. \quad (25)$$

B. Total Scattering and Absorption Invariance

The extinction, absorption and scattering cross sections for a system with dipole moments $|p\rangle$ and incident fields $|e\rangle$ are

$$\begin{aligned}\sigma_e &= \frac{k}{\epsilon_0\left|\mathbf{E}^0\right|^2}\mathrm{Im}\left\{\langle e|p\rangle\right\} \quad (26)\\ \sigma_a &= -\frac{k}{\epsilon_0{}^2\left|\mathbf{E}^0\right|^2}\left(\frac{k^3}{6\pi}\langle p|p\rangle + \mathrm{Im}\left\{\langle p|\left(\hat{\alpha}^{(6N)}\right)^{-1}|p\rangle\right\}\right)\\ \sigma_s &= \sigma_e - \sigma_a\end{aligned}$$

The rotational symmetry we introduced in the previous section is contained entirely within the inner product terms of the extinction and absorption cross sections, being $\langle e|p\rangle$, $\langle p|\hat{\alpha}^{-1}|p\rangle$ and $\langle p|p\rangle$. We will consider these inner products separately.

The first of the inner products, $\langle e|p\rangle$, can be expanded in terms of $\langle e_h|$ and $|p_h\rangle$ using (24) and (25)

$$\begin{aligned}\langle e|p\rangle = \langle e_h|\,&\alpha^2 + 2\alpha\beta a + \beta^2 a^2 + \beta^2 b^2\hat{\Pi}_n^{(6N)}\\ &+ \left(\alpha\beta b + \beta^2 ab\right)\left(\hat{R}_n^{(6N)}\hat{\Pi}_n^{(6N)} + \left(\hat{R}_n^{(6N)}\right)^T\right)|p_h\rangle\end{aligned}$$

The permutation matrices are then absorbed by $\langle e_h|$ using (18)

$$\begin{aligned}\langle e|p\rangle = \langle e_h|\,&\alpha^2 + \beta^2\left(a^2 + ab\left(\hat{R}_n^{(6N)} + \left(\hat{R}_n^{(6N)}\right)^T\right) + b^2\right)\\ &+2\alpha\beta\left(a + \frac{1}{2}b\left(\hat{R}_n^{(6N)} + \left(\hat{R}_n^{(6N)}\right)^T\right)\right)|p_h\rangle \quad (27)\end{aligned}$$

Now, because $|e_h\rangle$ is defined as having no component perpendicular to the n-fold axis, we can neglect all components of $\hat{R}_n^{(3)}$ along that axis and replace each $\left(\hat{R}_n^{(6N)} + (\hat{R}_n^{(6N)})^T\right)$ term with $2\cos\left(\frac{2\pi}{n}\right)\hat{I}^{(6N)}$. Then, by applying both (22) and (23), we are left with

$$\langle e|p\rangle \;=\; \langle e_h|\,\alpha^2 + \beta^2\,|p_h\rangle\,.$$

Finally, for a plane wave we note that

$$\alpha^2+\beta^2=\frac{1}{2N}\langle e|e\rangle=\left|\mathbf{E}^0\right|^2$$

and the expression then becomes

$$\langle e|p\rangle \;=\; \left|\mathbf{E}^0\right|^2\langle e_h|p_h\rangle\,. \tag{28}$$

The remaining two inner products in (27), $\langle p|\left(\hat{\alpha}^{(6N)}\right)^{-1}|p\rangle$ and $\langle p|p\rangle$, can be thought of as analogous cases of each other where $\hat{\alpha}^{(6N)}\to\hat{I}^{(6N)}$ and vice versa. So we will begin by expressing $\langle p|\left(\hat{\alpha}^{(6N)}\right)^{-1}|p\rangle$ in terms of $\langle p_h|$ and $|p_h\rangle=(\hat{M}^{(6N)})^{-1}\epsilon_0\hat{\alpha}^{(6N)}|e_h\rangle$ using (25)

$$\begin{aligned}\langle p|\left(\hat{\alpha}^{(6N)}\right)^{-1}|p\rangle=\langle p_h|\left(\hat{\alpha}^{(6N)}\right)^{-1}\Big[&\alpha^2+2\alpha\beta b+\beta^2a^2+\beta^2b^2\\&+\left(\alpha\beta b+\beta^2ab\right)\Big(\hat{R}_n^{(6N)}\hat{\Pi}_n^{(6N)}\\&+\left(\hat{R}_n^{(6N)}\hat{\Pi}_n^{(6N)}\right)^T\Big)\Big]\left(\hat{M}^{(6N)}\right)^{-1}\epsilon_0\hat{\alpha}^{(6N)}|e_h\rangle.\end{aligned}$$

Every $\hat{R}^{(6N)}\hat{\Pi}_n^{(6N)}$ term will commute with $(\hat{M}^{(6N)})^{-1}$ (a result of (17)) and thereafter the permutation matrices can be absorbed by $|e_h\rangle$

$$\begin{aligned}\langle p|\left(\hat{\alpha}^{(6N)}\right)^{-1}|p\rangle=\langle p_h|\left(\hat{\alpha}^{(6N)}\right)^{-1}\left(\hat{M}^{(6N)}\right)^{-1}\Big[&\alpha^2\\&+\beta^2\left(a^2+ab\left(\hat{R}_n^{(6N)}+\left(\hat{R}_n^{(6N)}\right)^T\right)+b^2\right)\\&+2\alpha\beta\left(a+\tfrac{1}{2}b\left(\hat{R}_n^{(6N)}+\left(\hat{R}_n^{(6N)}\right)^T\right)\right)\Big]\epsilon_0\hat{\alpha}^{(6N)}|e_h\rangle.\end{aligned}$$

Here the terms in the square parentheses are the same as in (27), and we have already shown that they reduce to $|E|^2$. As such $\langle p|\left(\hat{\alpha}^{(6N)}\right)^{-1}|p\rangle$ and, analogously, $\langle p|p\rangle$, can be expressed as

$$\begin{aligned}\langle p|\left(\hat{\alpha}^{(6N)}\right)^{-1}|p\rangle&=\left|\mathbf{E}^0\right|^2\langle p_h|\left(\hat{\alpha}^{(6N)}\right)^{-1}|p_h\rangle\\\langle p|p\rangle&=\left|\mathbf{E}^0\right|^2\langle p_h|p_h\rangle\,.\end{aligned} \tag{29}$$

Substituting (28) and (29) into our original expressions for the extinction, absorption and scattering cross sections (27) we get

$$\begin{aligned}\sigma_e&=\frac{k}{\epsilon_0}\,\mathrm{Im}\left\{\langle e_h|p_h\rangle\right\}\\\sigma_a&=-\frac{k}{\epsilon_0^2}\left[\frac{k^3}{6\pi}\langle p_h|p_h\rangle+\mathrm{Im}\left\{\langle p_h|\left(\hat{\alpha}^{(6N)}\right)^{-1}|p_h\rangle\right\}\right]\\\sigma_s&=\sigma_e-\sigma_a\end{aligned} \tag{30}$$

Noticeably the cross sections are independent of the coefficients α and β, which defined the generality of the incident field in (24). As such, we can conclude that the extinction, absorption and scattering cross sections will all be independent of the polarization in a linearly-polarized plane wave that is travelling parallel to the n-fold axis of a dipole system (for $n\geq 3$).

IV. EXAMPLES OF LIGHT SCATTERING

To demonstrate the validity of our approach we employed a number of methods to study the light scattering by some oligomer structures with n-fold symmetries [see Figs.2-4]. First, we applied analytical Generalized Mie theory [38, 39] for spherical particle clusters to calculate the exact total extinction, scattering and absorption cross-sections. Second, we used CST Microwave Studio to calculate the near-field profiles of corresponding structures. And, finally, we employed the dipole approximation and dyadic Green's function method to analyze optically induced electric and magnetic dipoles distribution of individual nanoparticles [37]. We should mention that all three approaches prove the polarization independence of optical properties, in accordance with our theoretical predictions. Moreover, these methods provide us with flexibility in analyzing the structures while maintaining a full understanding of the system. We used Palik's book for permittivity data of various materials used in this paper [40].

Figure 2 show the extinction, scattering and absorption cross-sections for a trimer consisting of three touching silicon nanoparticles of radii $R=75$nm. Figure 3 shows the extinction, scattering and absorption cross-sections for a heptamer consisting of seven gold nanoparticles with 6-fold symmetry. All particles of these oligomer-like structures are in the same transverse plane, so the excitation field is identical for all particles. We can also lower the symmetry of a structure by shifting some particles along the propagation axis. For example, in Fig. 4 we present a structure with 3-fold symmetry which was derived from a gold heptamer structure shown in Fig. 3. To construct the new structure we, first, shifted two equilateral trimers of the outer ring in opposite directions from the central particle evenly spaced along the propagation axis, and, then, twisted with respect to each other. The final structure appears to be chiral with 3-fold symmetry. Thus, according to our theoretical prediction we expect that it should be polarization invariant, which is numerically confirmed.

All structures exhibit polarization-independent optical properties for *any* incident polarization angle, which does not necessarily coincide with the rotational symmetry of the structures. These figures show that the total absorption is polarization-independent even though the near-field distribution varies with the incident polarization. It allows us to conclude, that, although, all structure exhibit some degree of geometrical anisotropy, their optical response is *isotropic* one. And the only requirement that we imply is that the structure supports n-fold symmetry with $n\geq 3$.

Based on the coupled dipole approximation method [41] the optical response of structures with *arbitrary* geometries and complex refractive index can be approximated by an ensemble of discrete dipoles. Thus, our results can be easily generalized to *any* structure with n-fold symmetry. Figure 5 shows the results of direct numerical simulations of a continuous structure with 3-fold symmetry for simplicity modeled as $\rho(\theta) = R[1 + \cos(1.5\theta)]$ with $R = 200$ nm (on the transverse plane) and $h = 100$ nm (along longitudinal direction) thick made of gold. It still exhibits polarization-independent optical response, in full agreement with our approach above. This proves that our statement is quite universal and can be applied to any system.

V. CONCLUSIONS

In conclusion, we have studied the optical responses of structures that possess an n-fold ($n \geq 3$) rotational symmetry under excitation from incident plane waves propagating parallel to the rotational symmetry axis. We have rigorously proven that polarization-independent responses (in terms of the cross sections of scattering, absorption and extinction) can come solely from the overall rotational symmetry of a structure without any conditions placed on other ingredients of a given system. Specific numerical examples have been demonstrated to follow these derivations. Such robust polarization-independent features are expected to play an important role in various applications including nanoantennas, sensing, imaging, solar cells and many other applications in biological and medical research.

ACKNOWLEDGMENTS

The authors thank Anton Desyatnikov, Andrey Sukhorukov, Dragomir Neshev and Yuri Kivshar for useful discussions. We acknowledge the support of the Australian Research Council Centre of Excellence for Ultrahigh bandwidth Devices for Optical Systems (Project No. CE110001018) and Future Fellowship (Project No. FT110100037).

---

[1] Y. W. Jun, S. Sheikholeslami, D. R. Hostetter, C. Tajon, C. S. Craik, and A. P. Alivisatos, P. Natl. Acad. Sci. **106**, 17735 (2009).

[2] N. Liu, M. Hentschel, T. Weiss, A. P. Alivisatos, and H. Giessen, Science **332**, 1407 (2011).

[3] A. V. Kabashin, P. Evans, S. Pastkovsky, W. Hendren, G. A. Wurtz, R. Atkinson, R. Pollard, V. A. Podolskiy, and A. V. Zayats, Nat. Mater. **8**, 867 (2009).

[4] L. Novotny and N. van Hulst, Nat. Photonics **5**, 83 (2011).

[5] A. G. Curto, G. Volpe, T. H. Taminiau, M. P. Kreuzer, R. Quidant, and N. F. van Hulst, Science **329**, 930 (2010).

[6] H. A. Atwater and A. Polman, Nat. Mater. **9**, 865 (2010).

[7] C. F. Bohren and D. R. Huffman, *Absorption and scattering of light by small particles* (Wiley, New York, 1983) p. xiv.

[8] U. Kreibig and M. Vollmer, *Optical properties of metal clusters*, Springer series in materials science (Springer, Berlin ; New York, 1995).

[9] Z. C. Ruan and S. H. Fan, Phys. Rev. Lett. **105**, 013901 (2010).

[10] L. Verslegers, Z. Yu, Z. Ruan, P. B. Catrysse, and S. Fan, Phys. Rev. Lett. **108**, 083902 (2012).

[11] X. J. Ni, N. K. Emani, A. V. Kildishev, A. Boltasseva, and V. M. Shalaev, Science **335**, 427 (2012).

[12] N. F. Yu, P. Genevet, M. A. Kats, F. Aieta, J. P. Tetienne, F. Capasso, and Z. Gaburro, Science **334**, 333 (2011).

[13] H. Noh, Y. Chong, A. D. Stone, and H. Cao, Phys. Rev. Lett. **108**, 186805 (2012).

[14] A. E. Miroshnichenko, S. Flach, and Y. S. Kivshar, Rev. Mod. Phys. **82**, 2257 (2010).

[15] B. Luk'yanchuk, N. I. Zheludev, S. A. Maier, N. J. Halas, P. Nordlander, H. Giessen, and C. T. Chong, Nat. Mater. **9**, 707 (2010).

[16] D. W. Brandl, N. A. Mirin, and P. Nordlander, J. Phys. Chem. B **110**, 12302 (2006).

[17] F. Hao, Y. Sonnefraud, P. V. Dorpe, S. A. Maier, N. J. Halas, and P. Nordlander, Nano Lett. **8**, 3983 (2008).

[18] M. Hentschel, M. Saliba, R. Vogelgesang, H. Giessen, A. P. Alivisatos, and N. Liu, Nano Lett. **10**, 2721 (2010).

[19] M. Hentschel, D. Dregely, R. Vogelgesang, H. Giessen, and N. Liu, ACS Nano **5**, 2042 (2011).

[20] N. S. King, Y. Li, C. Ayala-Orozco, T. Brannan, P. Nordlander, and N. J. Halas, ACS Nano **5**, 7254 (2011).

[21] J. Ye, F. Wen, H. Sobhani, J. B. Lassiter, P. Dorpe, P. Nordlander, and N. J. Halas, Nano Lett. **12**, 1660 (2012).

[22] M. Frimmer, T. Coenen, and A. F. Koenderink, Phys. Rev. Lett. **108**, 077404 (2012).

[23] A. B. Evlyukhin, C. Reinhardt, A. Seidel, B. S. Luk'yanchuk, and B. N. Chichkov, Phys. Rev. B. **82**, 045404 (2010).

[24] A. Garcia-Etxarri, R. Gomez-Medina, L. S. Froufe-Perez, C. Lopez, L. Chantada, F. Scheffold, J. Aizpurua, M. Nieto-Vesperinas, and J. J. Saenz, Opt. Express **19**, 4815 (2011).

[25] A. I. Kuznetsov, A. E. Miroshnichenko, Y. H. Fu, J. B. Zhang, and B. S. Lukyanchuk, Sci. Rep. **2**, 492 (2012).

[26] A. B. Evlyukhin, S. M. Novikov, U. Zywietz, R. L. Eriksen, C. Reinhardt, S. I. Bozhevolnyi, and B. N. Chichkov, Nano Lett. **12**, 3749 (2012).

[27] A. E. Miroshnichenko, B. Luk'yanchuk, S. A. Maier, and Y. S. Kivshar, ACS Nano **6**, 837 (2012).

[28] W. Liu, A. E. Miroshnichenko, D. N. Neshev, and Y. S. Kivshar, ACS Nano **6**, 5489 (2012).

[29] W. Liu, A. E. Miroshnichenko, D. N. Neshev, and Y. S. Kivshar, Phys. Rev. B. **86**, 081407 (2012).

[30] M. Rahmani, T. Tahmasebi, Y. Lin, B. Lukiyanchuk, T. Y. F. Liew, and M. H. Hong, Nanotechnology **22**, 245204 (2011).

[31] R. Shankar, *Principles of quantum mechanics* (Plenum Press, New York, 1980).

[32] P. R. Mcisaac, IEEE. T. Microw. Theory. **23**, 429 (1975).

[33] M. J. Steel, T. P. White, C. M. de Sterke, R. C. McPhedran, and L. C. Botten, Opt. Lett. **26**, 488 (2001).

[34] W. Liu, A. A. Sukhorukov, A. E. Miroshnichenko, C. G. Poulton, Z. Y. Xu, D. N. Neshev, and Y. S. Kivshar, Appl. Phys. Lett. **97** (2010).

[35] K. Aydin, V. E. Ferry, R. M. Briggs, and H. A. Atwater, Nat. Commun. **2**, 517 (2011).

[36] S. N. Sheikholeslami, A. Garcia-Etxarri, and J. A. Dionne, Nano Lett. **11**, 3927 (2011).

[37] G. W. Mulholland, C. F. Bohren, and K. A. Fuller, Langmuir **10**, 2533 (1994).

[38] Y.-l. Xu, Appl. Opt. **34**, 4573 (1995).

[39] M. Ringler, A. Schwemer, M. Wunderlich, A. Nichtl, K. Kürzinger, T. A. Klar, and J. Feldmann, Phys. Rev. Lett. **100**, 203002 (2008).

[40] E. D. Palik, *Handbook of Optical Constants of Solids* (Academic Press, 1997).

[41] B. T. Draine and P. J. Flatau, J. Opt. Soc. Am. A **11**, 1491 (1994).

[42] A. Miroshnichenko and Y. Kivshar, submitted (2012).

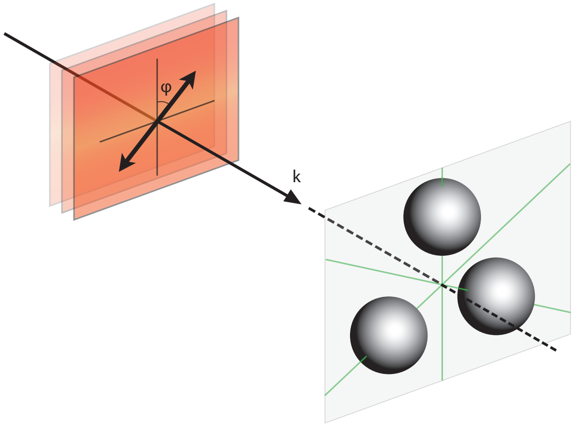

FIG. 1. Schematic view of the problem under consideration - linear polarised plane wave scattering by a system with rotational symmetry.

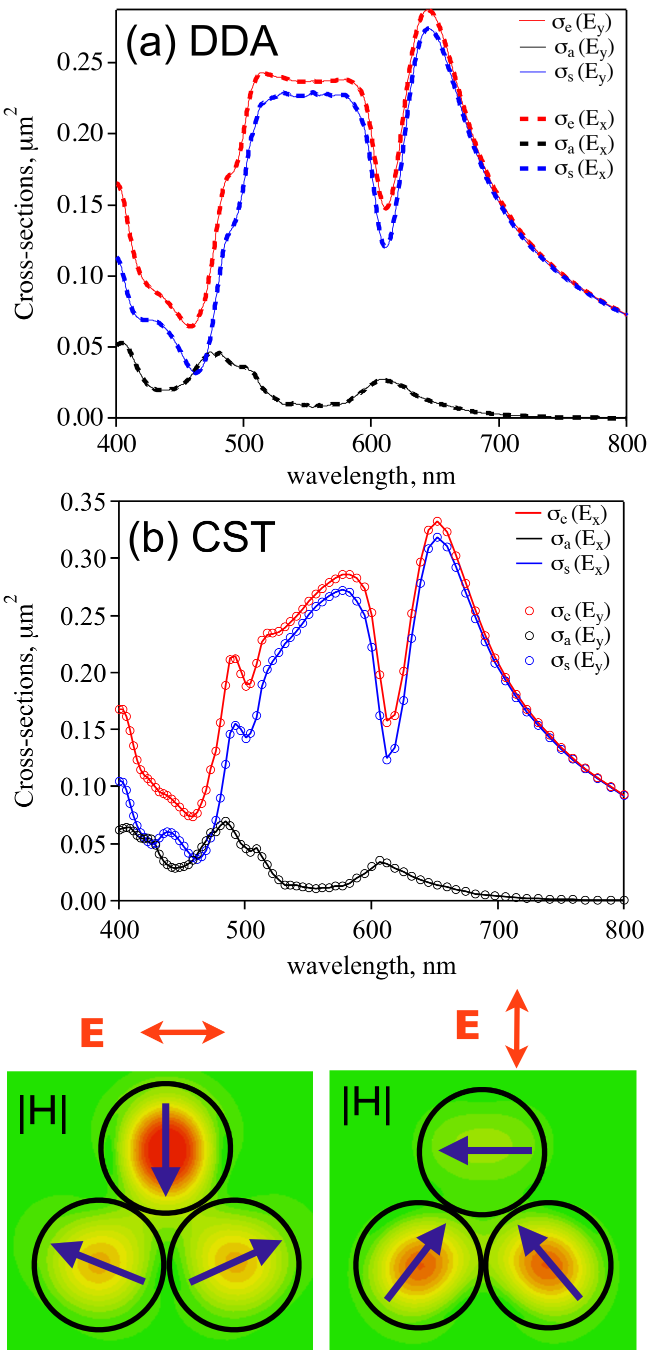

FIG. 2. Extinction, scattering and absorption cross-sections for two orthogonal polarizations for trimer structure made of touching silicon nanopartices of radii $R = 75$nm calculated by using (a) discrete dipole approximation (DDA) method and (b) by direct numerical simulations with CST Microwave Studio. Bottom panels show magnetic field distribution at the Fano resonance [42], $\lambda = 612$nm, for two polarizations together with induced magnetic dipole moments.

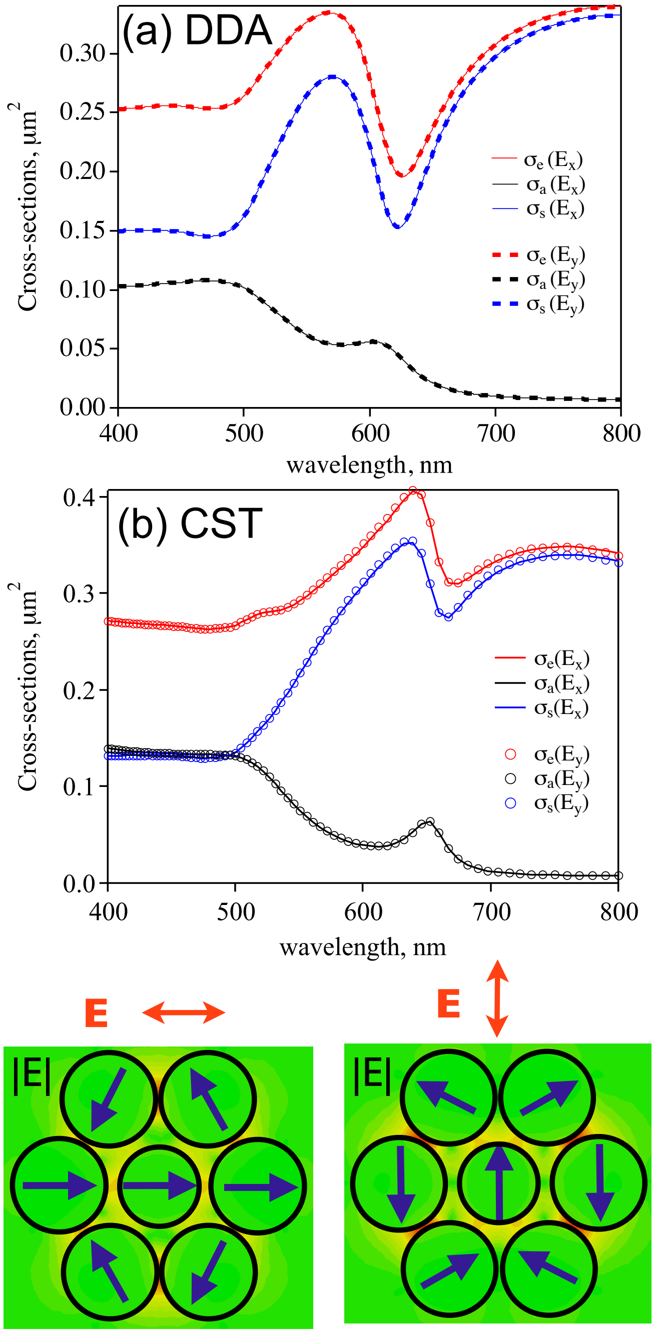

FIG. 3. Extinction, scattering and absorption cross-sections for two orthogonal polarizations for heptamer structure made of gold nanopartices of central $R_c = 65$nm and outer $R_o = 75$nm radii separated by $d = 10$nm calculated by using (a) discrete dipole approximation (DDA) method and (b) by direct numerical simulations with CST Microwave Studio.. Bottom panels show electric field distribution at the Fano resonance [18], $\lambda = 600$nm, for two polarizations together with induced electric dipole moments.

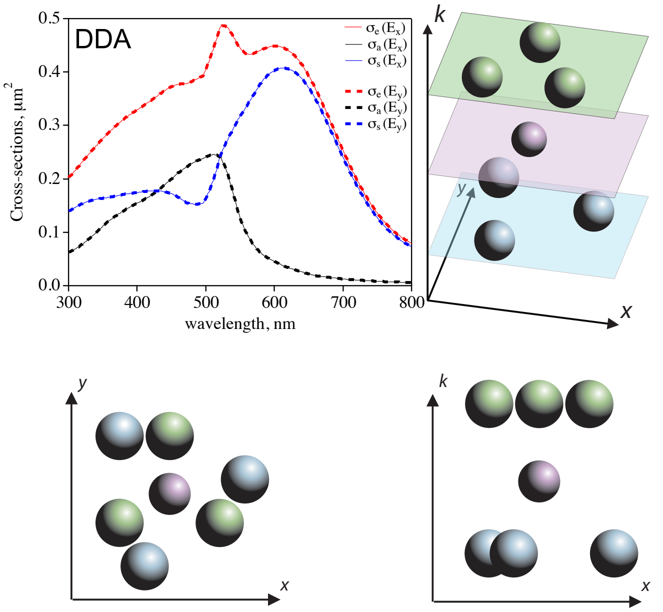

FIG. 4. Extinction, scattering and absorption cross-sections for a structure with 3-fold symmetry consisting of two equilateral trimers (marked by different colors) that are separated by a central particle and evenly spaced along the propagation axis. The trimers are also twisted with respect to each other in order to make the structure chiral.

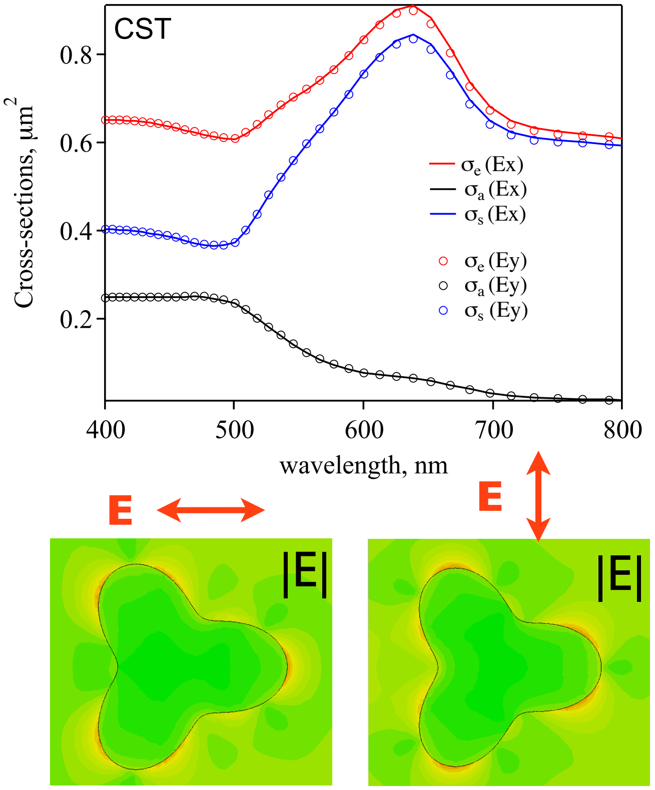

FIG. 5. Scattering and absorption cross-sections for continuous structure for two orthogonal polarizations with $n = 3$-fold symmetry.